Dynamics of a Large Spin-Stiffened Deployable Paraboloidal Antenna

JOHN M. HEDGEPETH*
Astro Research Corporation, Santa Barbara, Calif.

Very large deployable space structures are most efficiently stiffened by centrifugal forces caused by spin. One of the characteristics of such large spin-stiffened structures is a battery of structural dynamics problems that influence the system design to a much greater extent than ordinarily experienced. One such system is the LOFT, a low-frequency radio telescope that consists of a large-aperture (~1500 m) paraboloidal reflector. Results of some recent investigations of this configuration are reported.

Introduction

BECAUSE the space within the payload fairings of launch vehicles is limited, deployable structures are used to accomplish many tasks in space. Among the deployable structures presently being used are hinged, foldable ones, such as the Pegasus meteoroid panels, booms, such as the antenna elements on the Radio Astronomy Explorer satellite, and pressurized inflatable structures, such as Echo.

The examples given above are of course not inclusive of all the deployable structures that are presently in use. In addition, many more deployable concepts have been proposed which have not been realized in the form of flight hardware. One of these types is the rotationally deployed and stiffened structure, a structure which has no bending stiffness of its own but which derives all of its ability to withstand perturbation loads and maintain its shape from the effects of centrifugal forces. Such a technique can be expected to be useful because of the fact that it is the most efficient means of creating truly large, lightly loaded structures.

Structures many kilometers in diameter can be deployed through spin stiffening. However, such structures are susceptible to complex dynamic responses to exciting forces. Although the types of structural dynamics problems encountered are not new to the field (e.g., helicopter blades are subject to all of the types of centrifugal forces, Coriolis forces, and gyroscopic moments), the values of certain significant parameters are many orders of magnitude different from those previously encountered. A large, paraboloidal, low-frequency radio telescope (LOFT) is interest for future space applications and has received a great deal of analytical and experimental study.

This report deals with investigations of the dynamic characteristics of the LOFT. The concepts of construction, packaging, and deployment mechanisms are discussed. The important dynamic problems dealt with are deployment, vibration characteristics, response to excitation, and structural-control interaction.

Baseline Configuration of Loft

The LOFT concept was generated as a means of providing a high-resolution broad-band antenna system for radio-astronomical observations over the frequency range 10 MHz to a few hundred KHz. There are several approaches to developing such a system, including interferometry with widely separated simple antennas[1] and the use of large rhombic arrays.[2] The one chosen by radio astronomers for Earth-based instruments and the one that presumably is most desirable for space basing, if feasible, is the paraboloidal dish reflector. For beam widths of a degree or so at 10 MHz, an aperture of about a mile is required. Now, a paraboloidal dish 1500 m in diameter has a surface area of just under 2,000,000 m^2. Even if it were made of one-mil-thick aluminum foil, the dish would weigh 138,000 kg, obviously a prohibitive weight. Fortunately, since the wavelength of the electromagnetic radiation is large (>30 m), the reflecting surface can be made of a tenuous network of thin conductive tapes and still achieve high reflectivity and low leakage. Such reasoning has led to the design described in Ref. 3 and shown in Fig. 1.

The basic reflector derives its stiffness completely from centrifugal forces. The entire configuration spins around the axis of symmetry at a rate of one revolution every 11 min. Front stays are required to pull the network into the desired near-paraboloidal shape. The small tensile loads in these stays are reacted by a compression force in a half-mile-long deployable central compression column. The reflected electromagnetic energy is collected at the focal point of the paraboloid by a large broad-band feed antenna such as the pyramidal log-periodic feed shown in Fig. 1. Control of the pointing direction of the telescope is achieved by passing currents through the net and around the rim mass which serves the dual purpose of carrying the currents and providing a concentrated mass to react the inward components of the tension forces in the front stays and the reflector.

The reflector is not a true paraboloid; study of filamentary tension structures shows that such a shape is extremely difficult to achieve exactly. The LOFT reflector therefore is paraboloidal (with an f/d of 0.5) from the rim to the 50% of radius point, then is a tangent cone to the 40% point where a set of backstays is attached to enable the transition to a nearly conical surface of constant circumferential tension to the 20% point, and then a tangent cone to the axis. This shape is within 2m of a true paraboloid except for the innermost 10%, which, of course, comprises only 1% of the total area.

The reflector structure is composed of a structural support net with 240 meridionals and 40 circumferentials filled in with an aluminized polymer conductor grid that has a spacing of 40 cm. Details of these members are shown in Fig. 2. (0.1 in.-wide, $\frac{1}{4}$-mil polymer with 1000Å of aluminum vacuum deposited on both sides). The structural support members are trifilar for redundant resistance to meteoroids.

Further description of the structure, including the deployable column (which has received a great deal of investigation in its own right), the feed antenna, RF patterns, and

Presented at the ASME/AIAA 10th Structures, Structural Dynamics, and Materials Conference, New Orleans, La., April 14–16, 1969; submitted August 15, 1969; revision received April 1, 1970. This work has been supported by NASA under Contracts NAS7-426 and NAS5-11596.

* Vice President. Associate Fellow AIAA.

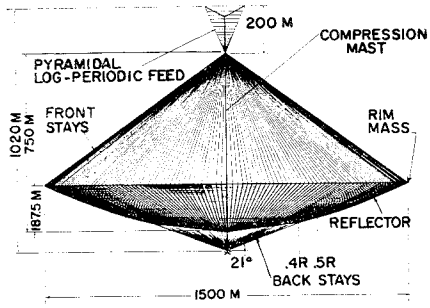

Fig. 1 Near-parabolic LOFT concept.

operational considerations, can be found in Refs. 3–9. The mass breakdown is shown in Table 1.

For a structure of its size, the load levels are extremely small. The total compression load on the central mast for example, is about 1.5 N (0.34 lb) and the stress in the structural members in the fully deployed state is of the order of 10 N/cm² (13 psi).

Packaging and Deployment Concepts

The packaged LOFT is shown in Fig. 3. The reflector net is wound onto a toroidal reel which can be envisioned as a circular bellows supported by a toroidal core. Each meridional structural support cable is wound into its own convolution in the bellows. A sprocket and chain drive system supplies torque to the toroid reel. The backstays are kept taut during packaging, deployment, and subsequent operation by means of a single storage reel. A similar reel is mounted to the front end of the centrally stored mast and is deployed as the mast is deployed. A rear mast is also required to position the backstay reel properly. Spinup power is provided by rocket thrusters mounted on the ends of small deployable columns. The over-all deployment sequence is shown in Fig. 4. Spinup is started, then the net is allowed to deploy into a plane. The central column is then extended to form the final configuration. This sequence is required in order to maintain stable ratios of moments of inertia of the spinning system.

Deployment Dynamics

When fully deployed, the LOFT telescope, even though it is very tenuous, possesses a tremendous amount of angular momentum because of its large size. The deployed moment of inertia is 227 × 10⁶ kg-m², and the rate of rotation is

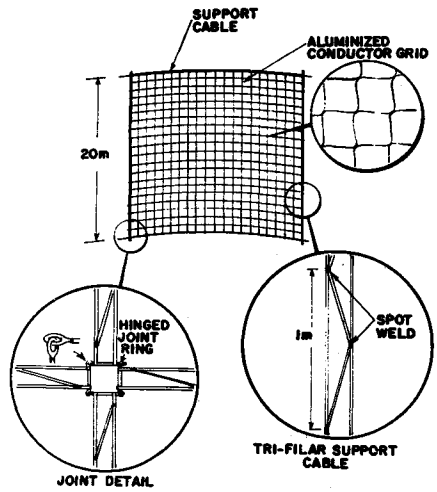

Fig. 2 Reflector structural detail.

Table 1 Mass breakdown

Support net	43 kg
Conductor grid	239
Backstays	12
Rim mass	227
Front stays	37
Main mast	250
Back mast	25
Feed system	200
Front-stay reel	50
Support structure, mast canisters	300
Toroid system	100
Backstay reel	50
Spinup subsystem	300
Power generation and storage	300
Control system	150
Data handling and communication	50
Launch shroud (portion chargeable to payload)	320
	2653 kg

0.0916 rad/sec, yielding an angular momentum of 2.08 × 10⁶ N-m-sec. The configuration starts with a diameter of ~4m and expands to a diameter of 1500 m. Clearly the problem of carrying out this deployment and at the same time storing the large amount of momentum into the system is a major one that requires detailed dynamic consideration. The rate at which the rocket thrusters provide spinup impulse has to be carefully synchronized with the rate of payout of the reflector net. Controlling this synchronization can obviously be a sensitive problem. The meridional members should not undergo excessive whipping; the angle at which they leave the toroid during unrolling should be controlled to an acceptable value to prevent tangling there; and when deployment is complete, the net should not have appreciable radial or tangential residual velocities.

In order to study the dynamics of deployment, one must construct a suitable model. The assumption has been made that all the meridional members behave exactly the same, and that the tensions in the circumferential members are small enough that their effect on the behavior of the meridionals is only due to their parasitic mass. Thus, the simplification can be made that the entire net behaves as a single massy string.

The equations of motion are hyperbolic and could be solved numerically by the method of characteristics. No solutions have been obtained as yet.

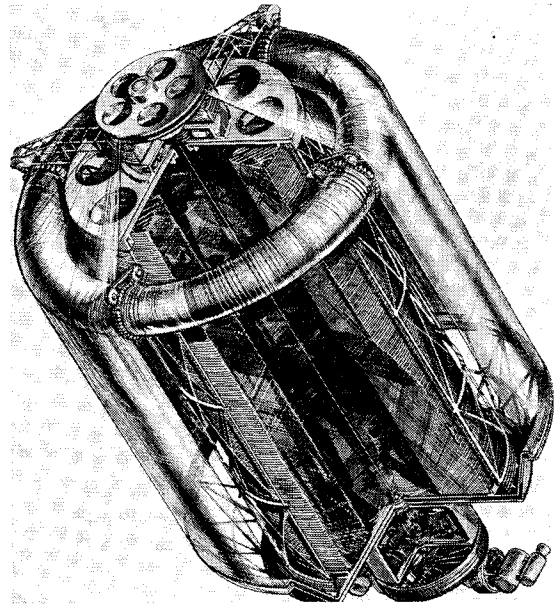

Fig. 3 Packaged LOFT.

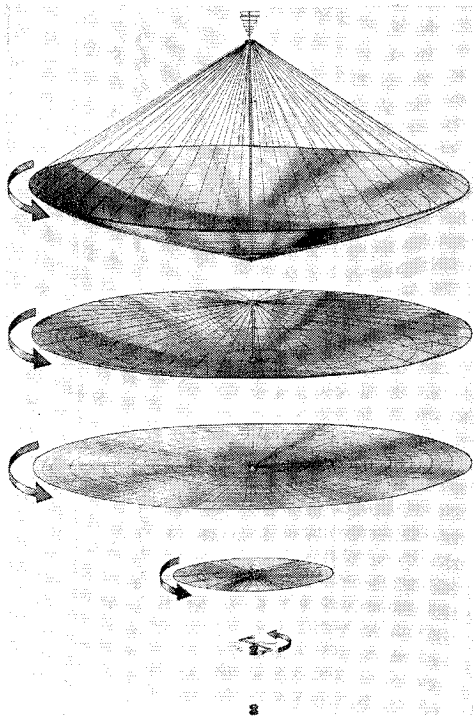

Fig. 4 Deployment sequence.

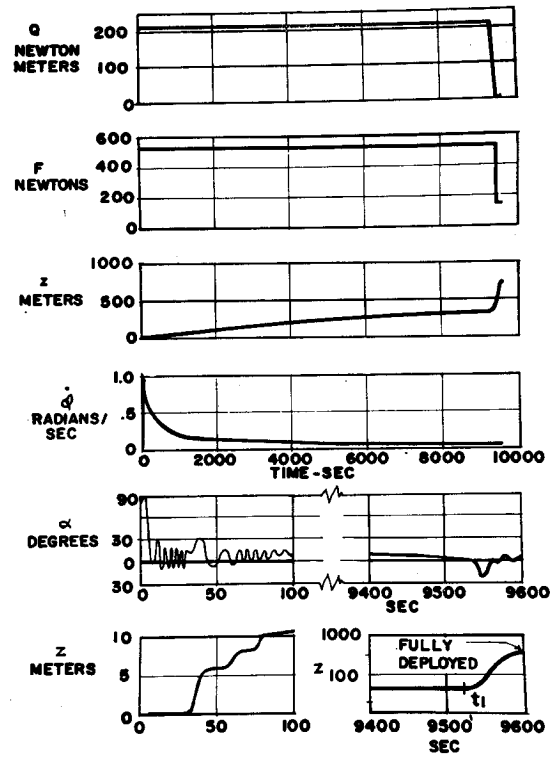

Fig. 6 Example results.

An approximate three-degree-of-freedom solution, however, has been carried out.[8] From the mass breakdown it can be seen that the rim mass is as large as the mass of the entire reflector net. Therefore, certainly in the limit of very slow deployment, the assumption can be made that the tip mass pulls so hard on the deploying string that the string is essentially straight. The three degrees of freedom therefore are (see Fig. 5): $z(t)$ = the deployed length of string at time, t; $\varphi(t)$ = the angle of rotation of the deployed string; and $\alpha(t)$ = the angle of trail of the deploying meridional from the toroid.

The rate at which these variables change will depend, of course, on the way in which deployment is controlled. One control parameter is the torque, Q, which is applied to the center body by the spinup rockets. Another control parameter could be either $z(t)$, the amount of deployment, or $F(t)$, the amount of force at the toroid reel to resist the unreeling of the meridional members. Both controlled-displacement and controlled-force types of deployment have been considered, and it has been found that a relatively simple "drag brake" type of control is feasible with a simple two-step scheduling of the spinup torque.

The equations of motion for this three-degree-of-freedom system were derived by the application of Lagrange's equations and solved numerically by the Runge-Kutta method. The main attention was given to the case where Q was constant and where the resisting force, F, was constant as long as the net was being stripped off, but was allowed to drop below this value when the net stopped paying out in order to prevent reversing of the reel. Because of the assumption that the meridionals remain straight, no investigation could be made of any possible whipping phenomenon, although it was shown, a posteriori, that for the cases of interest, the tension in the meridionals was indeed large enough to prevent excessive bowing due to Coriolis forces. Primary attention was paid therefore to the angle of trail α since the net would probably experience difficulties in being properly unreeled from the toroid if α exceeds 30°. The result of a sample calculation is shown in Fig. 6.

The torque was held constant until enough angular momentum had been stored in the system, then it was rapidly decreased to zero. The drag force was also held constant during this same time. At this point deployment was around 40% complete. Then the drag force was dropped to a level that allowed the net to complete deployment in such a way as to reach zero deployment velocity at the instant of full deployment. Transients were observed in the time histories of the various degrees of freedom at both the initiation of deployment and at the switching time. It was found that a sharp drop-off in torque produced an undesirable persistent α oscillation which was reduced to acceptable values by a ramp-type tailoff. Note that the rate of rotation φ

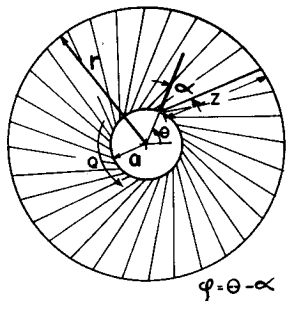

Fig. 5 Coordinates for approximate deployment analysis.

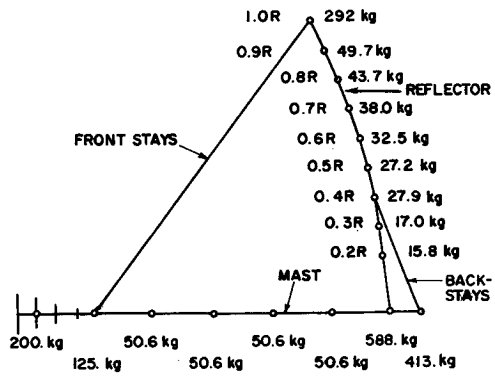

Fig. 7 Lumped mass, dynamic model.

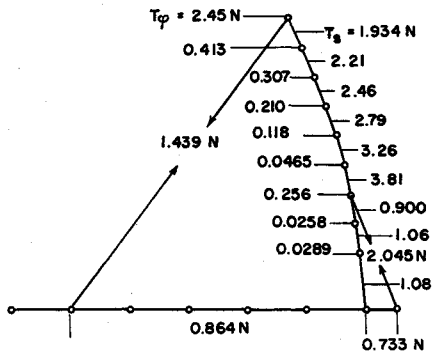

Fig. 8 Static load distribution.

rises very rapidly to relatively large values and then decreases monotonically to its final value. Note also that the majority of the total required deployment time is used during the first phase and that the final half of the deployment occurs in less than 1% of the total time. The drag force levels for this example were selected to give a stress in the meridional members of around 10,000 psi during deployment, and the torque level was selected to give an average trail angle of 10° during the initial phase.

Vibration Characteristics

The LOFT system, once deployed, is quite compliant, deriving all of its stiffness from the very small tensions which are created by the slow spin and small mast force. The first step in defining the dynamic characteristics of the structure is to determine the vibration modes and frequencies. Since the structure is axisymmetric, the vibration modes are sinusoidal around the circumference with integral wave numbers. Because of the rotation, the vibration modes are not standing waves but are traveling waves that have the general form $f(r)\ \exp(in\theta + i\omega t)$ as viewed by a body-fixed observer. For any particular wave number n there exist both a forward-traveling and a backward-traveling wave. The $n = 0$ modes include the rigid-body modes of axial translation and roll as well as various axial and torsional flexible modes. The $n = 1$ modes include the modes of pitch and yaw (which are not rigid-body because of the rotational effects) and the rigid-body modes of lateral translation. Also included are various flexible modes. The $n = 2$ and higher modes are all flexible modes and involve no mast bending.

The analysis[4,9] employs a Fourier decomposition in the circumferential direction and a discrete-mass consistent-displacement approach in the radial coordinate. The locations and magnitudes of the discrete masses are shown in Fig. 7.

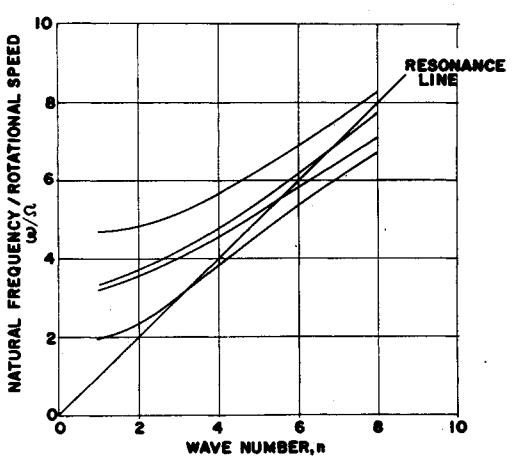

Fig. 9 Frequencies of backward-traveling waves.

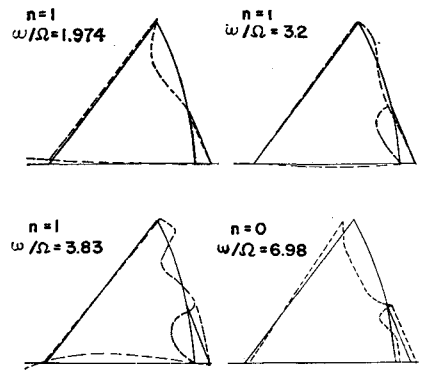

Fig. 10 First three reflector modes, backward-traveling waves; and first axial mode.

As has been mentioned, the configuration derives its stiffness primarily from the tensions. These tensions are shown in Fig. 8, where T_φ is the tension in the circumferentials associated with the mass station, and T_s is the total tension in all the meridionals connecting the mass stations. These tensions were converted to equivalent differential stiffnesses and entered into the SADSAM structural analysis computer program. Realistic compliances were introduced for the stretch of the members between mass points; subsequent analysis showed that the strain energy stored in these compliances in the centrifugal force field was about one thousandth of the total effective potential energy and was virtually inextensional except for the centrifugally bowed front stays.

The backward-traveling waves are of primary concern since they are likely to be excited by space-fixed disturbances. The variation of the body-fixed natural frequencies with circumferential wave numbers is shown in Fig. 9. Also shown is a 45° line which is the body-fixed frequency of a space-fixed static excitation. There is a near-resonance problem at $n = 3$.

It is clear that the natural frequencies must be very accurately predicted before flight, or there must be some means of adjusting the tension in flight so as to tune out an objectionable resonance situation. One means of doing this would be to control front and backstay tensions after deployment. Also, dampers could be mounted to the front and backstay reels to add damping to the system. This area constitutes a rich field for further study.

The shapes of some of the significant vibration modes are shown in Fig. 10. Note that the modes that involve primarily

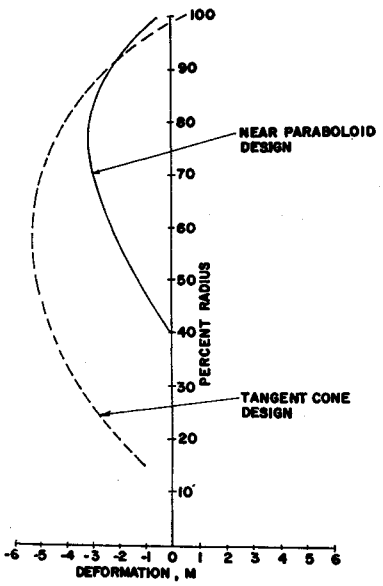

Fig. 11 Maximum distortions due to steady precessional moment of 135 N-m.

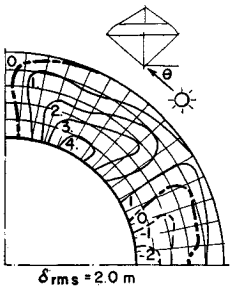

Fig. 12 Distortions due to solar heating (contour lines in meters).

reflector motion are characterized by a nearly fixed point at the intersection of the backstays and the net, but when column bending is induced, large motions at that point are observed.

Response to Excitation

The vibration modes and frequencies discussed in the preceding section can be used to calculate the response to the structure to external excitation. Two types of such excitation have been considered in detail; that caused by the application of control moments,[9] and that caused by nonuniform solar heating as the LOFT rotates.[4] These are the two most important sources. Order-of-magnitude analysis has indicated that the influence of gravity-gradient forces is an order of magnitude down from these and that the influence of solar pressure and meteoroid impact is still another order of magnitude lower. At the 6000-km design orbit the effect of atmospheric forces is even lower.

The largest control moment expected to be applied is that which will occur during the scan mode of operation of the telescope. In this mode the telescope will undergo a spiral scan of the celestial sphere and will be precessed about the orbital normal at a rate of once every 24 hr. This requires a moment of 135 N-m. This moment is applied by circulating currents around the rim and therefore the forces are applied locally there. As the telescope precesses, the motion of unforced portions of the net will tend to lag behind the rim; the amount of lag is of concern because of the influence of the distortion of the RF pattern of the telescope. Deflections of less than 2 m will produce less than one db degradation in performance. This acceptable 2-m value can be compared with the calculated response as shown in Fig. 11. The deflection is a maximum of 3 m, which occurs only over a low percentage of the total aperture.

As the LOFT rotates, its various structural members undergo varying temperatures. Results of calculations of thermal distortions, wherein the temperature at any time was assumed to be the radiation equilibrium temperature with an absorptivity/emissivity ratio (α/ϵ) of unity, are

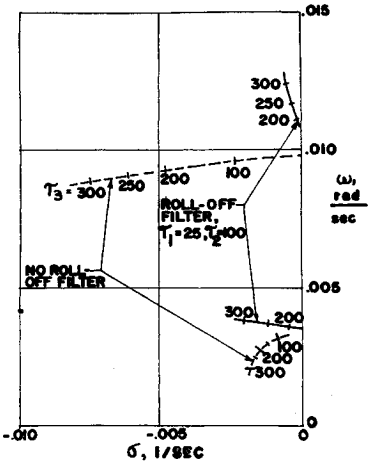

Fig. 13 Root-locus plot for rigid LOFT: τ_1, τ_2, and τ_3 are time constants in seconds (see text).

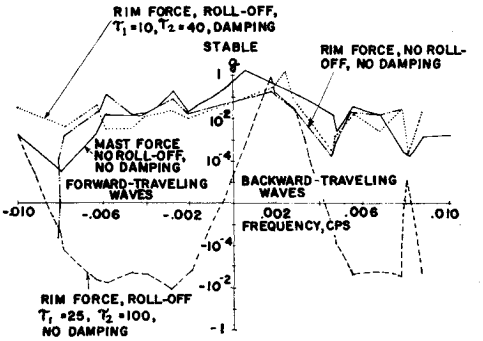

Fig. 14 Damping of coupled structure-control dynamic modes.

shown in Fig. 12 for the most severe sun aspect, which is tangent to the front-stay cone. These distortions are undoubtedly conservative because of the assumption of radiation equilibrium temperature. Some separate calculations have shown that the effects of including thermal inertia result in temperature variations much less than those calculated by the assumption of radiation equilibrium.

Interaction between Structural Flexibility and the Control System

Since the attitude of the LOFT telescope will be actively controlled, a primary problem of concern is the possibility of instability of the coupled system. In order to study the problem, it is necessary to characterize the control system to be used. As has been previously mentioned, two modes of active control are envisioned. One is the scan mode where the axis of symmetry is forced to track a predetermined path. The second is the "fixed mode" in which the axis of symmetry is commanded to point in a particular direction. In either case the control system can be considered to sense the departures of the axis of symmetry from the desired direction and to cause moments to be applied that will reduce the error. The studies[9] have employed the following simple control logic: 1) error angles and angular velocities are assumed to be measured with respect to a body system of coordinates that is fixed with respect to the line joining the ends of the central mast; 2) both error and rates are fed back. The gain on the error feedback was selected to be that required to produce an error angle of 0.1° if the largest gravity-gradient torque were applied steadily. Various values of rate feedback were considered; and 3) a second-order roll-off filter was assumed with varying time constants. The roll-off filter was felt to be required in order to minimize the influence of higher modes, particularly those involving motion between the sensors and the torque-applying devices.

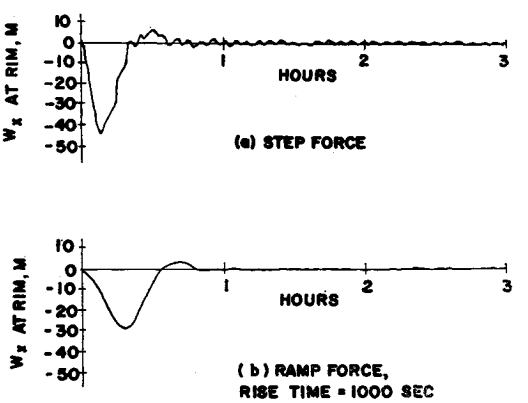

Fig. 15 Transient response to suddenly applied torque of 1750 N-m at rim.

The resulting control law is

$$\text{Moment} = K[(1 + \tau_3 s)/(1 + \tau_1 s)(1 + \tau_2 s)] \text{ (error angle)}$$

Rigid-Body Analysis

In Fig. 13 is shown a root-locus plot of the modes of motion of the LOFT considered to be a rigid body. Curves are shown for various values of lead time τ_3, for lag times of $\tau_1 = 25$ sec and $\tau_2 = 100$ sec, all for a displacement feedback gain of 10,000 N-m/rad. Also shown are the results if $\tau_1 = \tau_2 = 0$ (no roll-off filter). It can be seen that, as expected, the rate feedback characterized by τ_3 is stabilizing, but the roll-off filter is destabilizing. Other calculations indicated that if the gain were increased to 20,000 N-m/rad, the system with a roll-off filter would be unstable no matter how large the rate feedback. It was concluded from these studies that a value of $\tau_3 = 300$ sec should be used for the flexible-body calculations.

Stability of Flexible System

In the flexible system the location of the application of the control moment must be specified. Calculations were performed assuming that the control moment was applied at the tips of the central mast and at the rim of the paraboloid. The results are shown in Fig. 14 in the form of a plot of apparent damping coefficients as a function of frequency. It can be seen that if the roll-off filter is omitted and the moment is applied at the mast, the system is stable for all frequencies considered. Moving the location of torque application to the rim produces an unstable situation. The addition of a roll-off filter makes the system even more unstable at several frequencies. Even a relatively large amount of added damping, where the dampers are located at the intersection of the front stays and the central mast, does not completely eliminate the possibility of instability. An apparently stable situation can be obtained by decreasing the time constants in the roll-off filter in addition to adding damping.

Transient Response

A transient response analysis has been performed for a step-force and a ramp-force disturbance applied to the antenna at the rim for the stable control system with the reduced time constants in the roll-off filter. The results are shown in Fig. 15. It can be seen that if oscillations are created by transients, they tend to persist for a very long time. On the other hand, applying the force with a rise time of around 1.5 revolutions makes the amount of residual oscillation acceptable.

Concluding Remarks

On the basis of the studies conducted so far, the LOFT concept for constructing very large paraboloidal antennas appears quite feasible. It is, however, replete with problems, most of which involve some facet of structural dynamics. The influence of structural dynamics on the system design is therefore of paramount importance and must be accounted for throughout the development cycle.

References

[1] Taylor, G. E. and Hunter, J. R., "Structural Design and Operation of a Large Radio Astronomy Antenna," *Proceedings of the AIAA/ASME 9th Structures, Structural Dynamics and Materials Conference*, AIAA, New York, 1968.

[2] Crist, S. A., "Motion and Stability of a Spinning Spring-Mass System in Orbit," *Proceedings of the 8th AIAA/ASME Structures, Structural Dynamics and Materials Conference*, AIAA, New York, 1967.

[3] Schuerch, H. U. and Hedgepeth, J. M., "Large Low-Frequency Orbiting Radio Telescope," CR-1201, 1968, NASA.

[4] Engineering Staff, "Study of an Orbiting Low-Frequency Telescope," ARC-R-262, 1967, Astro Research Corp.

[5] Engineering Staff, "Preliminary Report on Gain Pattern Testing of RF Breadboard Models of LOFT," ARC-R-266, 1967, Astro Research Corp.

[6] Engineering Staff, "Design, Analysis and Testing of Models of an Orbiting Low-Frequency Telescope," ARC-R-268, 1967, Astro Research Corp.

[7] Engineering Staff, "Low-Frequency Telescope (LOFT) Final Report on Contract NAS7-426, Vol. I, Studies," ARC-R-300, 1968, Astro Research Corp.

[8] Hedgepeth, J.M . and Schlussler, L. G., "Deployment Dynamics of an Orbiting Antenna Packaged on a Toroidal Mechanism," ARC-LTN-16, 1969, Astro Research Corp.

[9] Engineering Staff, "Low-Frequency Telescope (LOFT), First Quarterly Report on Contract NAS5-11596," 1968, Astro Research Corp.